EVALUATION OF FORGING PARAMETERS ON Al-7075 AIRCRAFT DOOR BRACKET BY SIMULATION

E. Barati *and Kh. Farmanesh

* *Barati5@yahoo.com*

Received: February 2015 **Accepted: August 2015**

Department of Material Engineering, Malek Ashtar University, Shahin Shahr, Iran.

Abstract: *The purpose of this research is to achieve the optimal parameters for producing forged aluminium alloy 7075 aircraft door bracket by using finite element modelling (FEM) with commercial DEFORM-3D V6.1 and physical simulations with plasticine and Plexiglas dies. Also, forging speed has been examined as the main factor for controlling to produce a part without any defects. The results of Physical Simulation showed that the flow pattern has good agreement with the results of FEM that based on the use of hydraulic presses with initial billet and dies temperatures 410 and 400 ° C, respectively, and different forging speeds 5, 10 and 15 mm/sec. Distribution of effective strain rate, effective strain, effective stress, temperature , forging force and dies¬ wear showed improvement the results in forging speed of 5 mm/sec. Processing map of Aluminium alloy 7075 also checked out at constant strain 0.5, indicated that the specified area of the forged part is located in a safe area. Forging force in optimized forging speed 5 mm/sec showed that the forging process using a 1000-ton press can be done easily.*

Keywords: *FEM, 7075 Alloy, Physical Simulation, Forging Speed*

1. INTRODUCTION

Large plastic deformations, without a failure of formed parts, are possible in hot forging processes since flow stresses are dramatically reduced and work hardening not occur very much at elevated temperature. Therefore, hot forging processes are often used in the case of large deformations and limited capacity of press equipment because the flow stresses and forming energies are decreased at evaluated temperature. Aluminium alloys usually are widely utilized in automotive and aircraft industry due to their various advantages such as lightness, good forge ability, high wear resistance, etc. [1]. Among the highest-strength aluminium alloy, 7075 aluminium alloys, have highest strength and even in some cases as in Fig. 1 indicated that strength of 7075 aluminium alloys are higher than mild steels [2]. Forge ability of this alloy also is shown in Fig. 2, the 7075 aluminium alloys because of higher strength show very low forge ability [3]. Equation 1 related to the effective strain rate and deformation rate are expressed as follow:

$$\bar{\dot{\varepsilon}} = d[\ln \frac{(\frac{L}{L_0})}{dt}] = \frac{1}{L}\frac{dL}{dt} = \frac{V}{L} \quad (1) \qquad (1)$$

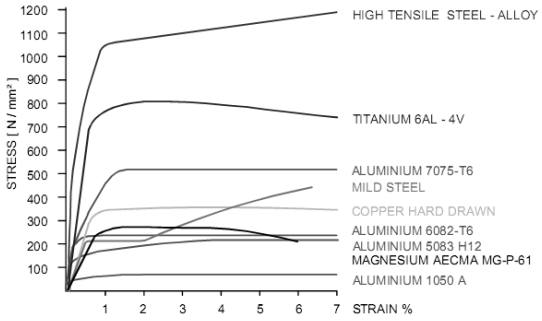

Fig. 1. Curves of stress - strain compared to aluminum, metals and alloys [2].

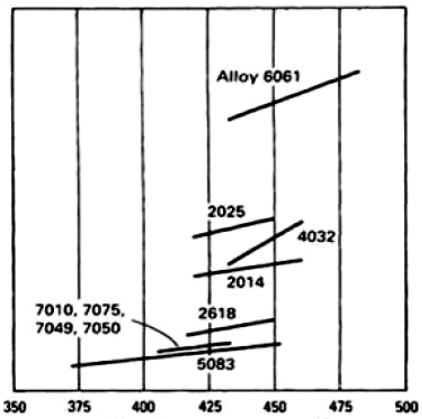

Fig. 2. Forgeability and forging temperatures of various aluminum alloys [3].

[Downloaded from www.iust.ac.ir on 2024-12-27]

[DOI: 10.22068/ijmse.12.4.51]

Equation 1 shows that if velocity (V) is fixed, with increasing length of the sample (L), the effective strain rate ($\dot{\varepsilon}$) decreases. As the strain rate increases, the extent of adiabatic heating in local regions increases significantly. Hence, in any particular region of the work piece, if the local strain rate increases above the nominal value, then it is accompanied by a reduction in the local flow stress. However, if flow stress increases with strain rate, then a very significant thermal softening will be encountered in the regime of high strain rates, which will produce severe strain localization and adiabatic shear bands [4]. Therefore, the deformation speed is very important in material forming process.

Quantitative analysis of the flow stress, the forming forces, the distribution of temperature and other process is necessary for successful design in hot forging processes. Thus forming conditions such as material properties, friction, lubricant, the effect of cooling rate, initial billet and dies temperature and flow stress, must be carefully considered [5,6].

Recently, FEM is a useful technique for design and select the appropriate operating conditions. Because of the strain rate sensitivity of the material at high temperatures, optimum hot forging visco-plastic analysis relationships are required [4]. In this study, according to equation 2 flow stress was considered as a function of strain, strain rate and temperature and on the DEFORM software environment, billet and dies behavior as a rigid-plastic and rigid material, respectively which the elastic deformer is ignored [7].

$$\bar{\sigma} = \bar{\sigma}(\bar{\dot{\varepsilon}}, \bar{\varepsilon}, T) \tag{2}$$

where $\bar{\sigma}$ mean effective stress and $\bar{\varepsilon}$ mean effective strain, $\bar{\dot{\varepsilon}}$ mean effective strain rate and T mean temperature.

plasticine is a material that is used to simulate the physical processes modeling. Mechanical behavior of plasticine at room temperature is very similar to the metals, especially steel at high temperature 1000°C [8]. If the lubrication conditions are chosen properly, the similarity in metal forming is completed. By using plasticine the stress distribution is similar to the stress distribution in metal forming [9].

Physical simulation is based on forming a low yield material compared to the original part in a format that can be made smaller or larger than it. Model of a material with a low yield stress, like plasticine, lead or wax is prepared. The die is made of an inexpensive material. Die are generally is made of mild steel, aluminum, wood or Plexiglas.

Due to lower costs, physical modeling in the forming processes design stages can be used for evaluate the process [10].

In this study, two methods, FEM and physical simulation were performed simultaneously and aluminum alloy 7075 Aircraft door bracket parameters at different forging speeds were studied. FEM were performed using DEFORM 3D V 6.1 software and for physical simulation plasticine clay and Plexiglas dies were used.

2. FORGING DIE DESIGN

In Fig. 3, 3D model of forged part after machining operations is shown. As can be seen, this part is composed of a Rib and Web sections. After designing a forging part, die forging according to the three-dimensional surfaces of the model was designed with CATIA V5R20. In Fig. 4, the longitudinal section of the upper and lower forging dies with position of the flash and gutter is shown.

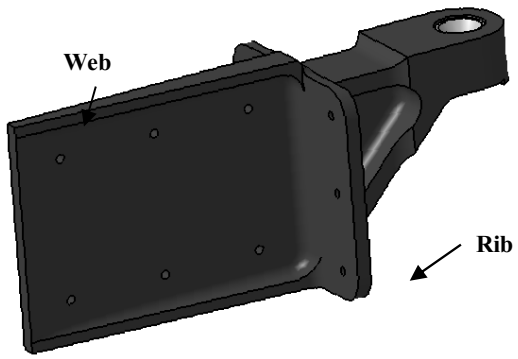

Fig. 3. 3D model of forged part after machining prepared by CATIA V5R20.

[Downloaded from www.iust.ac.ir on 2024-12-27]

[DOI: 10.22068/ijmse.12.4.51]

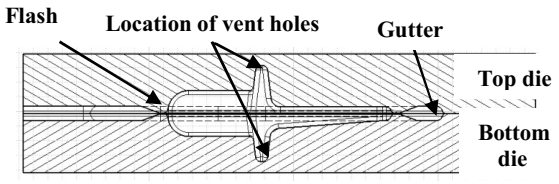

Fig. 4. Longitudinal section of the upper and lower die forging and location of Flash and Gutter designed by CATIA V5R20.

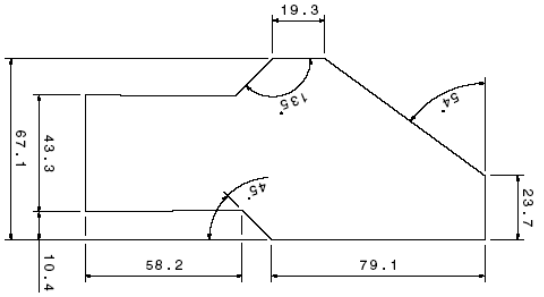

Fig. 5. Upper view of the designed billet by CATIA V5R20.

Table 1. General Characteristics of forging dies (mm)

The radius of Gutter to the die surface	The radius of the Flash connecto r die	Flash Gutter depth	Slope in Flash Gutter	Flash Widt h	Flash thickness
2	2	5	20	6	1

General Characteristics of die forging are shown in table 1. Due to the complexity of the part regarding design standards, Draft angle 7˚ were considered.

3. BILLET DESIGN

According to DIN7523, total mass of required material for forging is containing the total mass of flash and part after removing the mass of flash. Accordingly, the mass of billet based on table 2, by using of the CATIA V5R20 software is equal to 0.579 kg.

For designing the billet, it is assumed that forging operations is done by use of aluminum alloy 7075 flat bar section with standard size 1.5 inch X 3 inch. Then open die forging and machining operations or a combination of both is performed and required billet dimensions can be obtained. However, considering the size and weight of forged part billet forging design was done in CATIA V5R20 software. In Fig. 5, the image of the billet design with 30 mm in thickness is shown.

Table 2. Calculation of forging billet mass (kg)

Billet mass	Flash mass	Forging part mass
0.579	0.176	0.414

4. GENERAL SIMULATION CONDITIONS

The simulations have been carried out in accordance with SI units.

The material of dies is H-13 hot die steel and billet is Al 7075. The stress−strain relationships of aluminum alloy 7075 billet and H-13 die steel are selected from material library in the software DEFORM-3D. The physical properties and thermal boundary condition of these material are shown in table 3. In the simulation, the die was treated as a rigid body, while the billet was as a rigid-plastic material.

Table 3. Physical properties of materials and the thermal boundary conditions used in FEM modelling

Material	Heat transfer coefficient between work piece and dies (N/Scmm^2°C)	Heat transfer coefficient between work piece/dies and air/ (N/Scmm^2°C)	Emissivity ratio	Heat capacity/ (N/mm²°C)	Thermal conductivity/ (W·m−1·K−1)	Coefficient of thermal expansion/°C
Aluminium alloy 7075	11	0.02	0.1	2.43	180	2.2×10–5
H-13 Steel			0.3	3.0 (200 ℃)	24.6 (215 ℃)	1.22×10–5 (200 ℃)
				3.2 (315 ℃)	24.4 (350 ℃)	1.24×10–5 (315 ℃)
				3.8 (425 ℃)	24.2 (475 ℃)	1.30×10–5 (425 ℃)
				4.5 (530 ℃)		1.31×10–5 (480 ℃)

[Downloaded from www.iust.ac.ir on 2024-12-27]

[DOI: 10.22068/ijmse.12.4.51]

Table 4. Simulation parameters used in FEM

Loading speed of Male die/(mm·s−1)	Friction Factor	Initial temperature of die/℃	Initial temperature of billet/℃	Room temperature/℃
5,10,15	0.3	400	410	20

The shear friction model that is widely used in hot plastic FEM has been used to describe the friction at the interface. According to the friction between aluminum and steel alloys, the friction factor was considered 0.3 [11]. The thermal conductivity of aluminum alloy is much greater than of steel dies, and aluminum alloy is very sensitive to deformation temperature [12]. So, the Die was preheated up to close initial temperature of billet.

The simulation process was carried out in three different speeds that are summarized in table 4.

In this simulation, the absolute meshing of tetrahedral elements for the billet and the relative meshing for the dies have been used [13]. In relative meshing, number of elements is determined and number of elements during the simulation remains constant. Therefore due to geometry complexity of the part, the elements do not change. So that this properties are suitable for the dies that are rigid. But In absolute meshing, by increasing the complexity of the part, the specified element size is increased and these features enhances the simulation accuracy and according to the complexity of part the number of elements increases and this element meshing technique is appropriate for the billet. In order to improve the efficiency of the computation and prevent the destruction of meshes, automatic re-meshing technique is used [7]. For FEM, element size 1 and number of node and element 76946, 373664 were used, respectively.

For simulation the incremental lagrangian analysis was used.

5. PROCESS SIMULATION

In order to obtain a good agreement between simulation results and process results the process is divided into three operating stages:

a. Transfer billets from the furnace into a forging die.
b. Simulation of placing the billet on the lower die.
c. Forging process simulation, which includes downing of top die at a specific height (29 mm).

6. PHYSICAL SIMULATION

To perform physical simulation, Plexiglas dies and colored Plasticine was used. At this stage, based on the three-dimensional design by CATIA V5R20, CNC machining operations was performed on the Plexiglas. In Fig. 6, the images of Dies are observed. Due to limitations in placing the dies on hydraulic press, 4 guided pin, length 110 mm, as shown in Fig. 7, on the dies was made. Length of these pins enables the billet that can be easily placed on the lower die while the upper die is mounted on the pins and therefore there is no need to place the die close to the press, but the force on the upper die should be correctly loaded. plasticine layers in two different colors, white and orange in the same thickness 5 mm are placed on each other as shown in Fig. 8. The best lubricant, which can expressed the interface friction conditions to simulate the real conditions of forged 7075 aluminum, is soap suds [14]. Therefore, for physical simulation soap suds was used as a lubricant. Also, a small 63-ton hydraulic press at speed of 2 mm/sec at 25 °C was used in the specifications that are summarized in table 5.

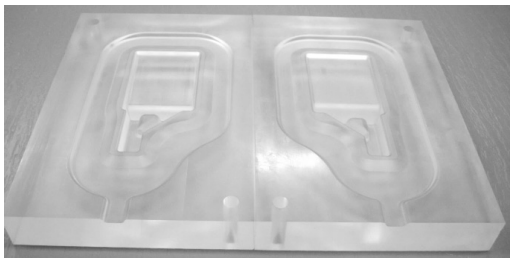

Fig. 6. Photograph of dies made by CNC machining for physical simulation.

[Downloaded from www.iust.ac.ir on 2024-12-27]

[DOI: 10.22068/ijmse.12.4.51]

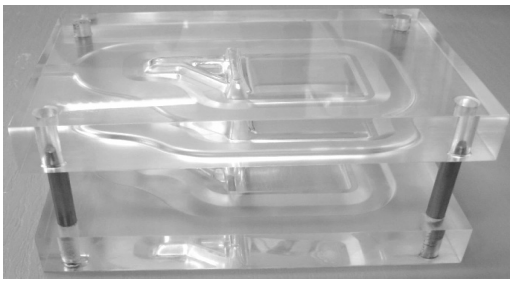

Fig. 7. Montaging of dies by using 4 pin guide.

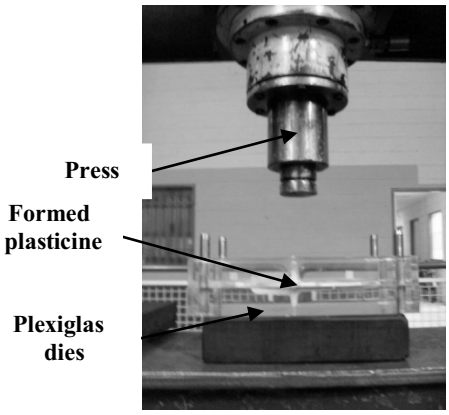

Fig. 9. Position at the end of the billet dies and physical simulation process.

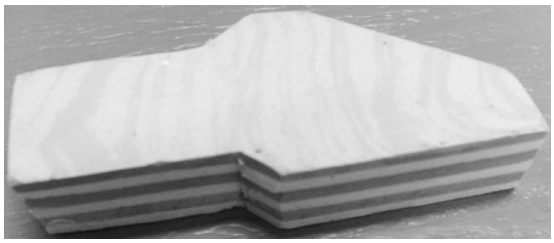

Fig. 8. Billet prepared using layers of colored pastes.

In Fig. 9, position of the billet on lower die at the end of simulation process is shown. After the physical simulation process, because the part is not axisymmetric, it was not possible to calculate the total strain distribution. So, strain was calculated from the rib zone. Cross-section of the rib is shown in Fig. 10. From it, flow pattern of the rib zone was achieved. Then, prepared sections, scanned and provided images, in subsection software CATIA Drafting, was entered and its thickness was measured by Equation 3, the strain distribution in each layer, assuming that the normal direction to the layers was considered a principal direction, were calculated[4,14].

$$\bar{\dot{\varepsilon}} = d[\ln \frac{(\frac{L}{L_0})}{dt}] = \frac{1}{L}\frac{dL}{dt} = \frac{V}{L} \quad (1) \qquad (3)$$

where $\bar{\varepsilon}$, is effective stress, h and , are the initial and final thickness of the plasticine layers, respectively.

Table 5. Specification of press, used in the physical simulation

Span Press	Diameter of piston	Maximum press course	Maximum allowable pressure	Press tonnage
1000 mm	100 mm	500 mm	150 bar	63 ton

7. RESULTS AND DISCUSSIONS

7.1. Evaluation of Die Filling

One of the most important results of successful forging is success die filling. Fig. 11, show the minimum distance of the die (from cross section

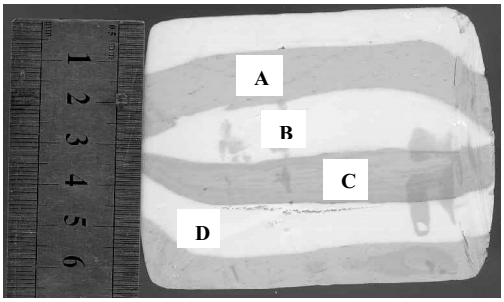

Fig. 10. Cross section prepared from Rib, to calculate strain.

[Downloaded from www.iust.ac.ir on 2024-12-27]

[DOI: 10.22068/ijmse.12.4.51]

of the rib zone) at a speeds 5, 10 and 15 mm/sec, which is predicted by the FEM. As can be seen, the minimum distance of material from the die at speeds of 5 and 10 mm/sec, is equal to zero, indicating that the dies are filled completely. At speed of 15mm/sec Minimum distance of die in a small area, is 0.45 to 1.8 mm Indicates that die is not completely filled. In Fig. 12, the filling of plasticine in Plexiglas dies, is showed. Fig. 13 has been shown top View from the forging part with the flash, prepared by two simulation methods - FEM and Physical. This figure offers the good agreement between the simulation methods. In Fig. 14, a comparison between the parts produced through physical simulation and FEM software DEFORM 3d V6.1 has been done. In this figure, good agreement between two samples is observed, indicating that the physical simulation is correct. Also, no apparent defects on samples obtained through physical simulation were observed.

7. 2. The Flow Pattern

In Fig. 15, the flow pattern of rib cross section obtained by FEM and Physical modeling has been compared. The results show the same flow pattern with a few difference that related to some dimensional errors.

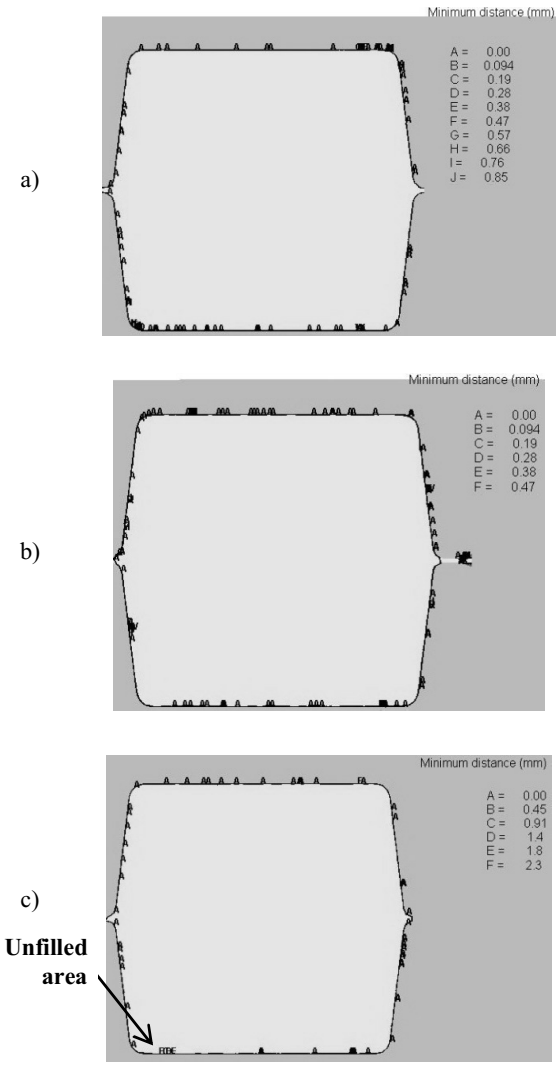

Fig. 11. Minimum distance to the speed of die forging, obtained by FEM a) 5mm/s, b) 10mm/s, c) 15mm/s.

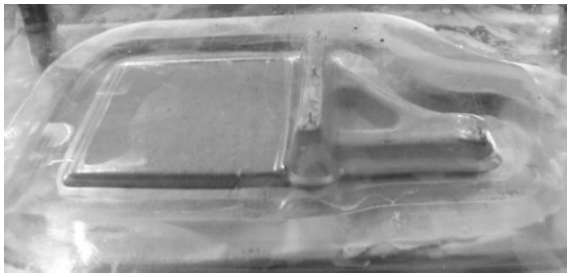

Fig. 12. Minimum distance to the speed of die forging 2mm/s obtained from the physical simulation.

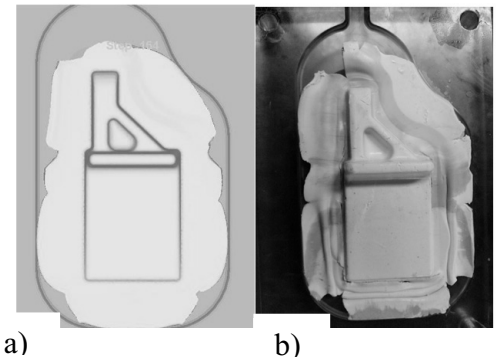

Fig. 13. Showing forged part with flash made of simulation: a) Physical b) FEM.

[Downloaded from www.iust.ac.ir on 2024-12-27]

[DOI: 10.22068/ijmse.12.4.51]

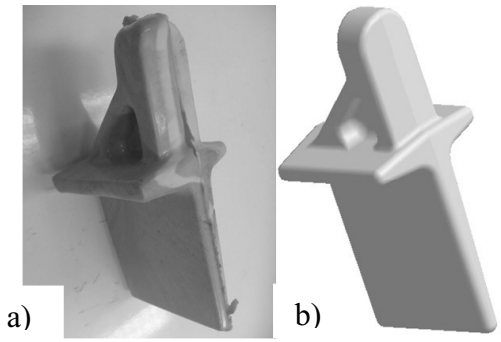

Fig. 14. Showing forged part made of simulation: a) Physical b) FEM.

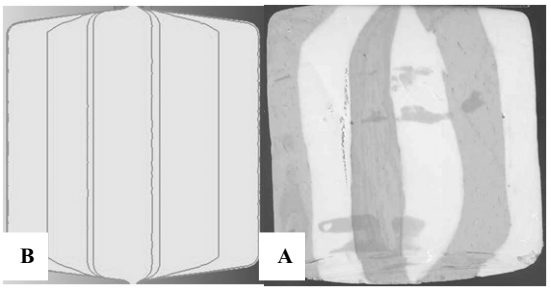

Fig. 15. Showing flow pattern made of simulation: a) Physical b) FEM.

7. 3. Distribution of Effective Strain

The strain distribution of the part, at three forging process speed, 5, 10 and 15 mm/sec, through FEM, (between points A and B in Fig. 16), is shown in the Figs. of 17 and 18. As can be seen, with increasing forging process speed, a significant change in the distribution of effective strain has not been reached. Temperature and rate of deformation, affect the flow stress. When the temperature increases, soft working mechanisms (recovery and recrystallization) are dominant that reduce the flow stress. In high Deformation speed, work hardening mechanisms are dominant which causes the flow stress be increased [4, 15]. Therefore, increasing Deformation speed, due to work hardening mechanisms dominate, the strain had not been changed. In order to determine the strain distribution in the cross sections of rib, in physical simulations, as noted assuming that the normal direction to the layers was considered a principal direction (Fig. 10), the strain distribution using the relation 3 were calculated that are summarized in table 6 [4, 14].

7. 4. Distribution of Effective Strain Rate

The effective strain rate distribution in three speed forging process 5 ,10 and 15mm/sec, using

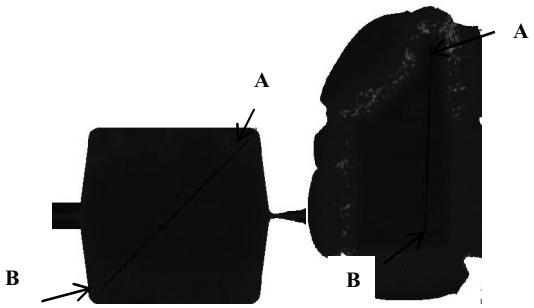

Fig. 16. Illustration the location of points A and B in the transverse and longitudinal sections of part.

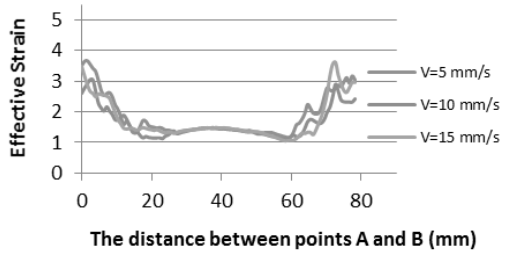

Fig. 17. Comparison chart of distribution of strain between points A and B in the cross section of rib.

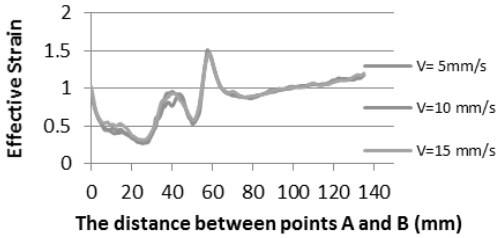

Fig. 18. Comparison chart of distribution of strain between points A and B in the cross section of web.

[Downloaded from www.iust.ac.ir on 2024-12-27]

[DOI: 10.22068/ijmse.12.4.51]

Table 6. Comparison of the calculated strain distribution in rib cross section by physical simulation and FEM

Specification of layer	FEM(5mm/s)	Physical simulatio (2mm/s)
A	1.6	1.3
B	1.23	1.3
C	1.49	1
D	1.27	1.1

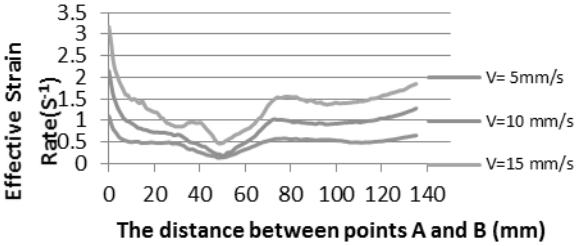

Fig. 20. Comparison chart of the distribution of strain rate between points A and B in the cross section of Web.

FEM (between points A and B in Fig. 16) has been obtained that are shown in Figs. 19 and 20,respectively. Can be seen that with increasing the deformation speed, the strain rate is increased. With increased Deformation speed, and dominate of work hardening mechanism, the strain rate is increased [4, 15].

7. 5. Stress Distribution

The distribution of the stress of the part at three speeds 5, 10 and 15 mm/sec, through FEM, (between points A and B in Fig. 16) have been obtained that is shown in Figs. 21 and 22 respectively. As can be seen, with increasing speed forging process, the effective stress in the rib cross sections is almost constant, but the effective stress in longitudinal section has a significant increase. The reason could be due to an increase in strain rate (previous section) and thus increase the amount of hard working in this area and increase flow Stress and thus may reduce hot workability.

7. 6. Temperature Distribution

The temperature distribution in the part for the three forging process speed of 5, 10 and 15 mm/sec, through FEM, (between points A and B in Fig. 16) have been obtained that are shown in Figs. 23 and 24, respectively. In the Figures a comparison between the temperatures distribution between points A and B at different speeds forging process has been done. With increasing Deformation speed and knowing that 98% of energy appears as heat, increasing in temperature can be clear [4, 15].

7. 7. Check the Forging Force

In this section, the effect of process speed on the required force to perform the forging process has been investigated. In the Figs. 25, the forging load at speed of 5, 10 and 15 mm/sec are compared. In table 7, the values predicted by the

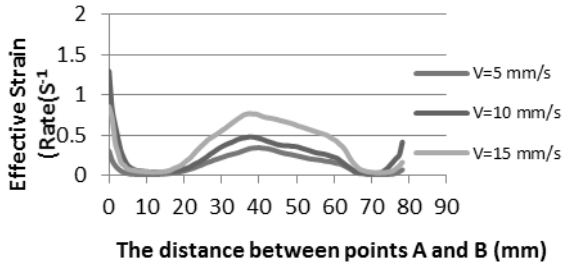

Fig. 19. Comparison chart of the distribution of strain rate between points A and B in the cross section of rib.

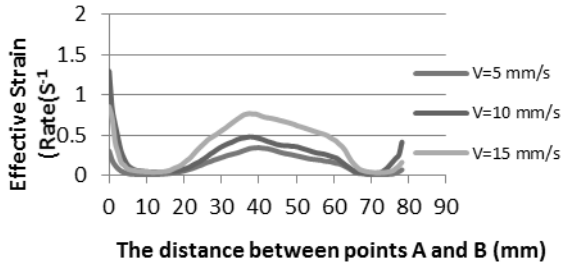

Fig. 21. Comparison chart of the distribution of stress between points A and B in the cross of Rib

[Downloaded from www.iust.ac.ir on 2024-12-27]

[DOI: 10.22068/ijmse.12.4.51]

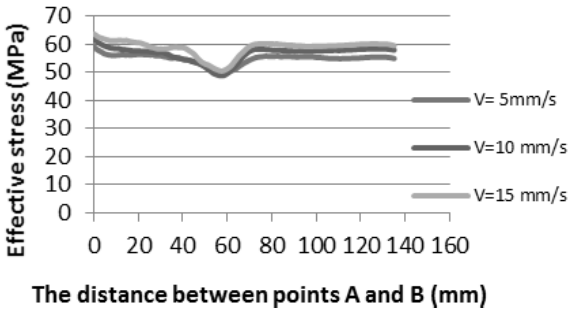

Fig. 22. Comparison chart of the distribution of stress between points A and B in the cross of web.

forging force has been given. As shown in Figure 25 and table 7, with increasing forging speed, required forging force, increases. According to the study, effective strain rate and effective stress in the previous sections and the increase in these two parameters, increasing Deformation speed, the force required for forging increases.

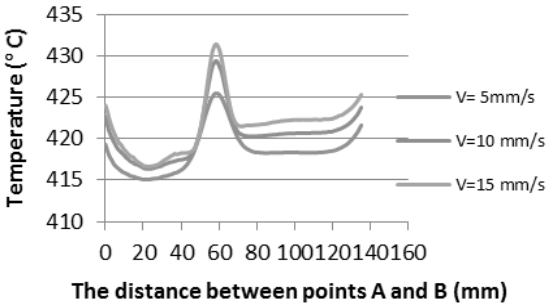

Fig. 23. Comparison chart of the distribution of temperature between points A and B in the cross of rib.

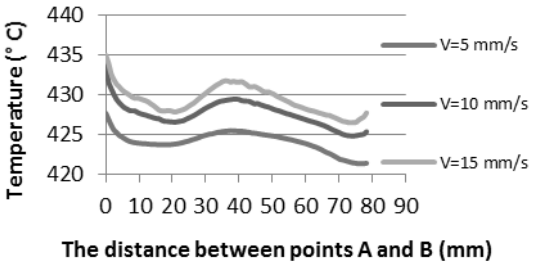

Fig. 24. Comparison chart of the distribution of temperature between points A and B in the cross of Web.

7. 8. Select the Optimal Forging Speed

Research has shown that stable flow conditions for hot forming of aluminum alloy 7075 are done at strain rate range of 0.001-1 S-1 and temperature range 300-500 °C [16,17] and at strain rates higher than 1 S-1 and temperatures below 450 °C unstable flow occurs[16-18]. As the strain rate increases, (speed forging 10 and 15 mm per second), the extent of adiabatic heating in local regions increases significantly. Hence, in any particular region of the work piece, if the local strain rate increases above the nominal value, then it is accompanied by a reduction in the local flow stress. However, if flow stress increases with strain rate, then a very significant thermal softening will be encountered in the regime of high strain rates, which will produce severe strain localization and adiabatic shear bands. [4]. Based on the above findings and the distribution of effective strain (Figs. 17 and 18), the distribution of temperature (Figs. 23 and 24),

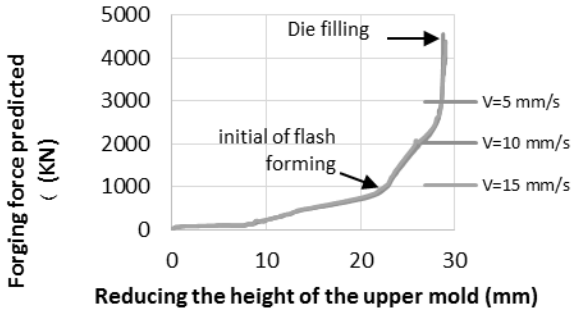

Fig. 25. Comparison chart of forging force at different speeds.

Table 7. Comparison of forging forces at different speed calculated by FEM

Forging speed(mm/s)	Forging force(KN)
5	4040
10	4390
15	4380

[Downloaded from www.iust.ac.ir on 2024-12-27]

[DOI: 10.22068/ijmse.12.4.51]

at different forging process speeds, we can easily see that ,stable flow are provided in forging speed of 5 mm/sec due to the strain rate range of 0.04-0.9 S-1and temperature Range 415-427 °C. Comparison of stress distribution in forging speed of 5 mm/sec with other speeds shows that with increasing temperature, flow Stress move towards the lower values (59-48 MPa), that results to increase workability[4]. On The other hand, Fig. 27 shows that the amount of energy for forging process with a speed of 5 mm/sec is smaller than others (4040 kN) the least forging forces decrease the amount of die wear and can reduces the cost of Tooling. The results in Table 7 show that the forging process can be performed by a 1,000 tons press easily.

8. COMPARISON OF SIMULATION AND EXPERIMENTAL RESULTS

In this section, simulation results performed in a specified area of the part is shown in Figure 26, and has been compared with the experimental results expressed in table 8.

The results in table 8 indicate that results of FEM on 7075 alloy aircraft door bracket have a good agreement with the experimental results.

9. CONCLUSIONS

The forging process of aluminum alloy 7075 aircraft door bracket was evaluated using FEM and physical simulation. The main results are as follows:

1. Physical Simulation results showed that the process of forging with designed dies and billet is possible at one pass and require no additional Pre-forming process.
2. Filling the die in physical simulation and FEM proved.
3. Flow pattern Cross section of plasticine by physical simulation has good agreement with the model obtained through FEM.
4. FEM based on the use of hydraulic press at the billet and die temperature, 410 and 400 °C respectively and a rate of 5 , 10 and 15 mm/s was done and process speed of 5mm/sec due to the distribution of strain rate effective 0.04-0.9S-1and temperature Range 415-427 °C , according to research, flow stability has dominated and Also has low flow stress and higher ductility and lower rates of forging force, Which reduces die wear and therefore, will reduce the cost of tooling, so as optimized forging process speed, is introduced.
5. In the specified area of the part, Comparison of results from FEM with experimental results has been performed that indicate the accuracy of the calculated results from simulations.
6. FEM results indicate that forging process by a1, 000 tons press is possible.

Fig. 26. Illustration of specified area used for conformation.

Table 8. comparison between results of FEM with experimental results in speed processing of 5mm/s for specified area in Fig 26.

Results	Temp. (°C)	Flow Stress (Mpa)	Strain rate (s^{-1})	Strain	Ref.
Simulation	420	54	0.27	0.54	FEM
Experimental	450	52	0.1	0.5	[17]
	450	50.6	0.1	0.5	[18]

REFERENCES

1. Kim, Y. H., Ryou, T. K., Choi, H. J., Hwang, B. B., “An analysis of the forging processes for 6061 aluminium-alloy wheels”. Journal of Materials Processing Technology 123, 2002, 270–276.
2. Cobden, R. and Banbury, A., " Aluminium: Physical Properties, Characteristics and

[Downloaded from www.iust.ac.ir on 2024-12-27]

[DOI: 10.22068/ijmse.12.4.51]

Alloys", TALAT Lecture 1501, EAA - European Aluminium Association, 1994, 44-60.
3. "Metals Handbook-Forming and Forging", Vol. 14, 9th Edition, ASM Handbook Committee. USA, 1988, 530-535.
4. Dieter, G. E., Kuhn, H. A. and Semiatin, S., L., editors, Handbook of Workability and Process Design, ASM International, 2003, 213-231.
5. Biswas, S. K. and Knight, W. A., "Perform design for closed die forging: experimental basis for computer aided design", Int. J.Mach. Tool Des. 1975, 15, 179–193.
6. Akgerman, T. A., "Recent developments in computer-aided design of forging process", SME Technical Paper, 1972, 72–110.
7. FLUHRER J. DEFORMTM 3D Version 6.1 User's Manual, MColumbus: SFT Inc., 2007.
8. Erman, E., and Semiatin, S. L., "Introduction-physical modeling of metalworking processes" Phisical Modeling of Metal Working Processes; Proceeding of a Symposium by the TMS-AIME and Forming Committee and held TMS annual meeting in Denver, 1987, 24-27.
9. Kim, H. Y., Kim, J. J. and Kim, N., "Physical and numerical modeling of hot closed-die forging to reduce forging load die wear", J of Material Processing Technology, 1994, 42, 401-420.
10. Mandić, V., "Physical modelling And fem simulation of the hot bulk forming processes", Journal for Technology of Plasticity, 2002, 41-53.
11. Sofuoglu, H., Gedikli, H. and Rasty, J., " Determination of FrictionCoefficient by Employing the Ring Compression Test" Journal of Engineering Materials and Technology, 2001, 123, 338-348.
12. Shan, D. B., Xu, W. C., Lu, Y., "Study on precision forging technology for a complex-shaped light alloy forging". J. Journal of Materials Processing Technology, 2004, 151, 289–293.
13. Hartley, P., Pillinger, I., "Numerical simulation of the forging process", Comput. Methods Appl. Mech. Engrg. 2006, 195, 6676–6690
14. Assempour, A. and Razi, S., "Determination of Load and Strain-Stress Distributions in Hot Closed Die Forging Using the Plasticine Modeling Technique", IJE Transactions B: Applications, 2002, 167.
15. Siegert, K., Möck, A. and Neher, R., "Forging Alloys", TALAT Lecture, 1994, 3401, 2-17.
16. Yang, Y., "The effects of grain size on the hot deformation and processing map for 7075 aluminum alloy", Materials and Design, 2013, 51, 592–597.
17. Rajamuthamilselvan, M., Ramanathan, S., "Hot deformation behaviour of 7075 alloy", Journal of Alloys and Compounds, 2011, 509, 948–952.
18. Prasad, Y. and Sasidhara, S., "Hot working guide: a compendium of processing maps", Materials Park, OH, ASM International, 1997, 142-147.

[Downloaded from www.iust.ac.ir on 2024-12-27]

[DOI: 10.22068/ijmse.12.4.51]